Desalination and Water Treatment
www.deswater.com

doi: 10.5004/dwt.2018.21974

108 (2018) 81–89
March

A theoretical study of a compact distillation module used in solar desalination unit

Khalifa Zhani[a,b]

[a]*Mechanical department, College of Engineering, University of bisha, Kingdom of Saudi Arabia, email: kzhani@ub.edu.sa*
[b]*LASEM (Laboratoire des Systemes Electro-Mecaniques), National Engineering School of Sfax, B.P. W3038, Sfax, Tunisia*

Received 10 June 2017; Accepted 4 February 2018

ABSTRACT

Water scarcity in several parts of the world is a matter of concern for human beings. Humidification–dehumidification (HD) solar desalination system is one of the viable approaches to mitigate the lack of fresh water. This paper focuses on the design and performance improvement of a distillation module used in a recent developed solar HD desalination system. The design and the principle of functioning of the distillation module are described. The influences of operating variables on yield and performance are studied. Operating variables include the air and water temperatures at entry to the distillation module, the humidifier water flow rate, and the cooling water flow rate into the dehumidifier. To conduct such a study, a mathematical model was established including the mechanism of heat and mass transfer in both the humidification chamber and the dehumidification one. These models use real meteorological data to predict the performance of a thermal solar-driven distillation module.

Keywords: Solar desalination; Humidification–dehumidification; Modeling; Simulation

1. Introduction

Water is indispensable for life but its availability is not assured everywhere. The earth contains about 1.4×10^9 km^3 of water, which covers approximately 70% of its surface area; the percentage of salt water in this large amount is 97%. The remaining 3% is fresh water with 70% of this amount frozen in the icecaps or combined as soil moisture. Both forms are not easily accessible for human use. 29% of all fresh water is underground, most of it in deep, hard-to-reach aquifers. The remaining quantity, about 1%, is believed to be adequate to support all life on Earth. So, fresh water can become a great problem since the water resources are limited and the problem will be aggravated by the exponentially growing demand for water due to progressive urbanization, industrialization process and growing population. It is expected that by the year 2025 more than 60% of the world's population will be faced with water shortage problems [1]. To cope with this issue and to respond to increasing water demand, desalination of seawater, which is abundant, is being considered.

The common desalination processes include multi-stage flash, multi-effect distillation, vapor compression and reverse osmosis (RO). However, they are economically only for large scale applications ranges of 100–50,000 m^3/d of fresh water production and still surfing being energy-intensive techniques, which consume high grade energy such as gas, electricity, oil, and fossil fuels. These processes lead to carbon footprints, which causes depletion of ozone layer as well as health hazards on mankind. It also leads to global warming which is the burning topic and becomes threat to life sustainability. In some circumstances, it is required to have a water desalination unit that do not exceed a few m^3/d. This decentralized demand favors local water production by developing desalination processes with low energy consumption as well as easy for handling and maintenance. In addition, the new trend in all energy required processes are directed to be driven whether fully or partially by renewable energy resource (solar, biogas, biomass gasification, geothermal, etc.). Solar humidification–dehumidification (HD) technique is one of the important methods of utilizing solar energy for the supply of fresh water to small communities where sunshine is abundant. In this technique, simply, the saline water is heated up to 60°C–90°C. Also the carrier air is heated using solar energy. Then water is misted and brought to contact with a stream of hot dry air. Thus the air is humidified up to saturation with water vapor. The saturated air is forced to pass through a cold condenser resulting in separating the fresh water from the air stream.

HD desalination plants are the most effective units among solar desalination plants. Many researchers have conducted studies on process and the equipments related to the HD systems for water desalination. Mashaly et al. [2] evaluated the application of solar energy to the desalination of water of different feed water quality levels for near zero liquid discharge under hyper arid environment. They investigated the influence of meteorological parameters on the performance of the solar still. They also determined during the desalination process the system productivity, operational recovery ratio, and thermal efficiency. It was found that the solar desalination system's performance depends to a great extent on solar radiation, ultraviolet, and the TDS concentration of feed water.

Attia [3] studied a solar desalination system using parabolic dish to heat up the working fluid in a closed space. Then the generated pressure in this space used to push salt water into RO module. It was found that the suggested system increases the productivity for each m^2 of solar radiation collecting surface. The productivity reaches up to 1.833 m^3/m^2 d at low operating pressure (brackish water). The productivity decreases with the increase of operating pressure, where at 80 bar, it becomes about 0.055 m^3/m^2 d which is suitable for sea water desalination. The suggested system gives a large quantity of production rate of fresh water with respect to other solar desalination system. And it is also suitable for remote areas at different types of water source.

Ghazal et al. [4] have developed a novel solar humidification technique incorporating the heating of water, the heating of the air stream and the humidification of air in one compact unit in order to improve the performance of solar HD systems while at the same time reducing the size of the whole system.The air is driven into the humidification unit in the form of bubbles and the effects of water temperature, bubble coalescence, bubble regeneration, and increased radiation by reflection on its performance has been studied. It was found that for an average intensity of solar radiation of 700 W/m^2 and a mass flow rate of 12.6 kg/h of air; the amount of water evaporated was 0.75 kg/h on a square meter basis and the introduction of a reflector mirror at the bottom side of the humidifier increased the average absolute humidity by 32%.

Many works were carried out to enhance the ability of the dehumidifier in solar desalination systems. A study has been investigated with a double pipe and shell and tube heat exchanger in a HD desalination unit and noticed the superior potential with shell and tube dehumidifier. Also, the study has extended to access the condenser adequacy with the effect of spring inserts. Spring inserts enlivened the condenser heat transfer coefficient and productivity [5]. Tow and Lienhard [6] observed the accelerated total heat flux and decreased effectiveness in the bubble column dehumidifier with the increase in air flow rate and temperature. A bubble column dehumidifier has been investigated by varying the pressure, water level and superficial velocity of air. It has been found that the total heat transfer rate and effectiveness enhanced with the hike in superficial velocity of air [7]. A plate fin tube dehumidifier for HD desalination has numerically analyzed and the performance is reported in detail [8].

Many types of humidifiers such as spray towers, bubble columns, and packed bed towers are commonly used. Kassim et al. [9] focused numerically the effect of inlet air humidity on an upward airflow in a humidifier intended for a HD desalination system. A vertical parallel-plate channel constitutes the humidifier. One of the plates is wetted by a liquid water film and maintained at a constant temperature, while the other is dry and thermally insulated. The airflow enters the channel with constant temperature, humidity, and velocity. It was found that the increase of air humidity at the channel entrance affects seriously the performances of the humidifier as it induces condensation of the water vapor on the walls. On the other hand, it was stated that the humidifier works well for low inlet humidity. Bourouni and Chaibi [10] studied theoretically heat and mass transfer in a horizontal-tube falling-film condenser used in an innovative desalination plant. The polypropylene exchanger was designed to work at, relatively, high temperatures (25°C–35°C). The elaborated model is based on the resolution of heat and mass transfer equations in each cell of the exchanger. The predicted transfer characteristics obtained from the simulations were compared with experimental data. The influence of the different thermal, hydrodynamic, and geometric parameters on the condenser performances was investigated. It was found that an increase in condensing exchanger performance when the inlet cooling water decreases and air velocity increases. For the conditions corresponding to the real environment of southern Tunisia, the model predicted that the amount of condensed water cannot exceed 2 m^3/d. Two types of air humidifiers, namely a tubular spray humidifier and a pad humidifier were experimentally compared and simulated as a part for a multiple stage solar desalination process by Yanniotis and Xerodemas [11]. They demonstrated that the pad humidifier is the most efficient and is more suitable than others for use to enrich air with water vapor in the new desalination process.

The developed solar desalination system that uses the HD principle includes four components; water and air solar collectors, humidifier and the distillation module. In two previous papers [12,13], we have presented the detailed study of the air and water solar collectors and the humidifier. In this paper, a new design for a distillation module is developed. The design includes the integration of the humidifier and the dehumidifier in a single compact module. This will significantly improve the mass and heat transfer process and allow for a longer contact time between water and air. In addition, this design displays a lower pressure drop and lower heat losses than with the separated humidifier and dehumidifier and allows for easier maintenance and cleaning of the distillation module. The performance of the proposed distillation module is investigated at different operating variables.

2. Mechanism of humidification and dehumidification

Solar desalination by HD process is based on the fact that air can carry considerable quantities of water vapor up to saturation. The amount of vapor able to be carried by air increases with the temperature; in fact, 1 kg of dry air can carry 0.5 kg of water vapor and about 670 kcal when its temperature increases from 30°C to 80°C [14]. The solar HD system mainly consists of a distillation module (humidifier and dehumidifier). In addition to this, water and air heaters are used to improve the capacity of the system. The distillation module is the most complicated component of the solar HD desalination unit since it involves the two reverse physical phenomena (humidification and dehumidification). Furthermore, the HD process is actually a multiphase flow, with phase change and simultaneous mass and heat transfer between the phases. The heat transfer between water and air can be divided into two categories according to the direction of mass transfer, heat transfer with humidification (evaporation) and heat transfer with dehumidification (condensation). Figs. 1(a) and (b) represent a schematic sketch for the mechanism of the interaction between the gas and liquid in both cases of HD states. In both figures, the broken arrows represent the diffusion of the vapor through the gas phase, and full arrows represent the flow of heat (both latent and sensible) through gas and liquid phases. The HD states have the following differences: (i) in humidification, the heat and mass move in opposite directions while in dehumidification they have the same direction; (ii) the vapor enters the interface at the water temperature in case of humidification while it enters the interface at the air temperature in case of condensation; (iii) the air film is thicker in case of evaporation but thinner in case of condensation; (iv) condensation commences when the partial pressure of water vapor in the air phase is higher than the partial pressure at the interface while evaporation commences when the partial pressure of water vapor at the interface is higher than the corresponding partial pressure in the air phase.

3. Distillation module design

Figs. 2 and 3 present the design and the experimental setup of the distillation module. The latter consists of air humidifier (evaporation chamber) and dehumidifier (condensation chamber). There is no wall separating the two chambers. In order to ensure a long-term operation of the distillation module, the evaporation chamber and the condensation chamber are well designed and realized. The condensation chamber is constituted of 12 dismantled vertical rows, to ensure its maintenance, arranged in triangular arrangement. Each row contains 12 circular tubes in copper of inner diameter 12 mm and outer diameter 14 mm, their length is 1.5 m. The transverse and the longitudinal pitch are designated, respectively, by 50 mm and 50 mm. The evaporation chamber consists of 12 horizontal tubes made of copper with inner diameter

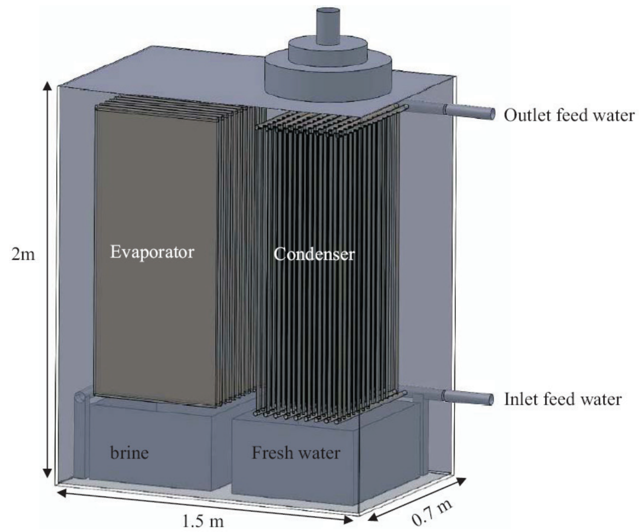

Fig. 2. Schematic diagram of the compact distillation module designed with Solidworks software.

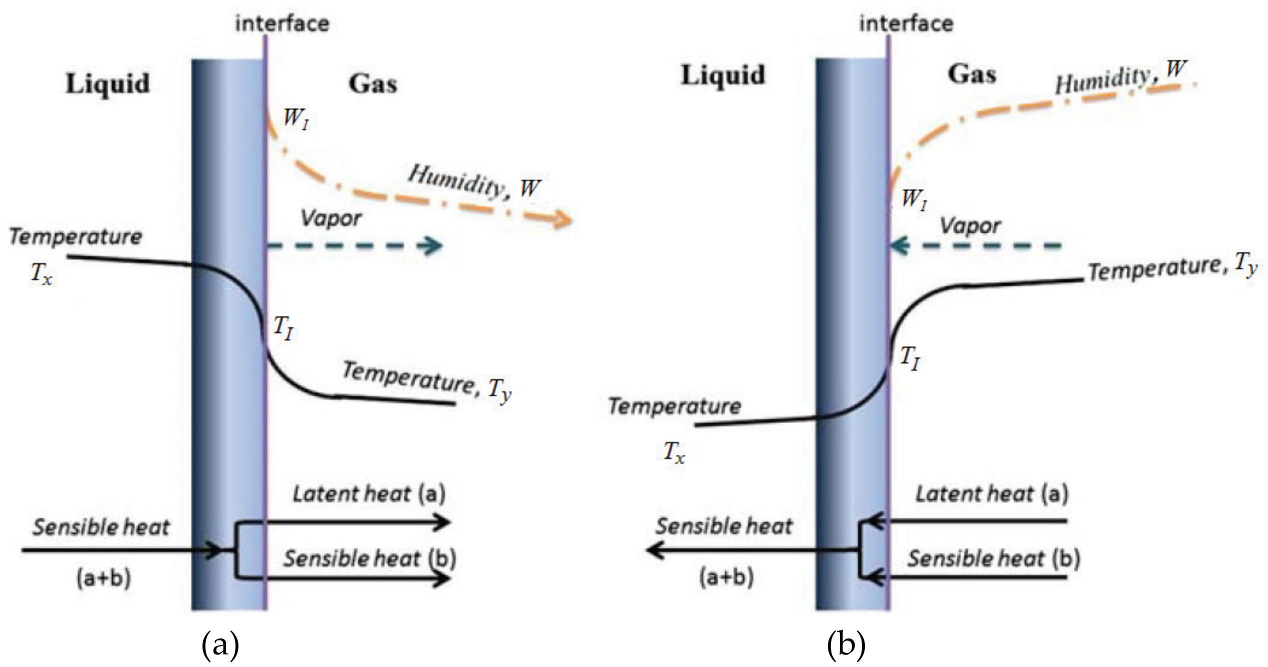

Fig. 1. Heat and mass transfer with humidification (a) and with dehumidification (b) [15.16].

Fig. 3. Outside and inside photos of the realized distillation module.

20 mm and outer diameter 22 mm equipped with small holes (1.5 mm diameter) provided on the higher surface of the tube. The holes work as pulverisers that pulverises the hot salt water. To augment the contact surface between air and water, thus, to increase the evaporation rate and to prevent pulverized hot salt water at the top of the evaporation chamber to be mixed with the fresh water at the bottom of condensation chamber, each horizontal tube mentioned previously, is covered with textile of exchange surface 49 m².

The principle of functioning of the distillation module is as follows: hot salt water coming from the water solar collector enters the module at the top of the evaporation tower. It is absorbed by the packed bed (textile of viscose). Due to heat and mass transfers between the hot water and the partially dehumidified air stream exiting the condensation tower at the bottom, air is loaded with moisture. The saturated moist air is then drifted towards the tower of condensation by natural convection where it enters in contact with a surface temperature of which is lower than the dew point of the air. The natural convection occurs when a solid surface is in contact with a fluid of different temperature from the surface. Density differences provide the body force required to move the fluid. The condensed water was collected from the bottom of the condensation tower, while the brine (the salty water exits the evaporator and the humidifier) at the bottom of both the humidifier and evaporation tower will be either recycled and combined with the feed solution at the entry point or rejected in case of increase of saltiness rates.

4. Mathematical formulation

The first stage of all survey of a thermal process requires its representation by a mathematical model. This model must characterize the real behavior of the studied system.

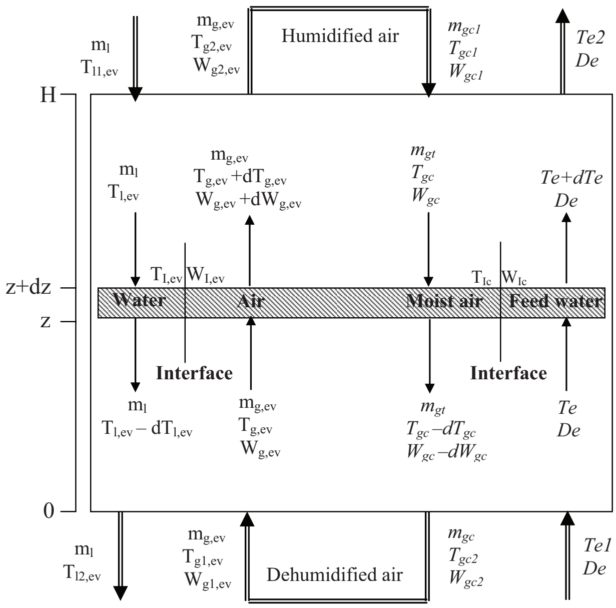

Fig. 4. An element of volume of the distillation module.

The distillation module may be modeled as shown in Fig. 4. Air flow rate enters the bottom of the evaporation chamber at a temperature $T_{g1,ev}(t)$ and a humidity $W_{g1,ev}(t)$. The mass velocity of air is $m_{g,ev}(t)$. The air flow rate exit at the top of the evaporation tower at a temperature $T_{g2,ev}(t)$ and a humidity $W_{g2,ev}(t)$. Hot water coming from water solar collector is pulverized at the top of the tower with a temperature $T_{L2,ev}(t)$ and no evaporated water is in the bottom of the tower with a temperature $T_{L1,ev}(t)$. The mass velocity of water is $m_l(t)$. The humid air, in provenance from the evaporator, enters the condenser by the top at temperature $T_{gc2}(t)$, humidity $W_{gc2}(t)$, and mass flow rate $m_{gt}(t)$. The cooling water is introduced at the bottom of the condenser at temperature $T_{e1}(t)$ and a mass flow rate $D_e(t)$.

The method of setting up the heat and mass balances will be undertaken with the following simplifying assumptions:

The process is adiabatic,

- The air and water flows are in countercurrent and one-dimensional,
- The specific heat of water is constant during its passage by the distillation module,
- The humid air is considered as a perfect gas.

4.1. Humidification process

4.1.1. Water phase

[Quantity of energy accumulated in the height volume element dz] = [(Quantity of heat carried away by water during dt) – (Quantity of heat transmitted toward the surface of separation water–air, during the same time dt)]

Mathematically, this can be expressed as

$$\frac{\partial T_{l.\text{ev}}}{\partial t} = \frac{m_l}{M_{l.\text{ev}}}\frac{\partial T_{l.\text{ev}}}{\partial z} - \frac{h_l a_{\text{ev}}}{M_{l.\text{ev}} C_l}\left(T_{I.\text{ev}} - T_{l.\text{ev}}\right) \quad (1)$$

4.1.2. Air phase

[Quantity of energy accumulated in the volume height element dz] = [(Quantity of heat received by the surface of separation water–air during the interval of time dt) – (Quantity of heat transmitted toward the debit of air during the same time dt)]

Mathematically, this can be expressed as:

$$\frac{\partial T_{g.\text{ev}}}{\partial t} = -\frac{m_{g.\text{ev}}}{M_{g.\text{ev}}}\frac{\partial T_{g.\text{ev}}}{\partial z} - \frac{h_g a_{\text{ev}}}{M_{g.\text{ev}} C_{g.\text{ev}}}\left(T_{g.\text{ev}} - T_{I.\text{ev}}\right) \quad (2)$$

4.1.3. Air–water interface in the humidification part

At the air–water interface, the thermal balance can be written under the following shape:

[Quantity of heat transmitted from the water current through the liquid film towards the surface of separation water–air] = [(Quantity of heat transmitted from the surface of separation through the air film toward the air current) + (heat quantity provided to evaporate the water mass quantity transferred of the liquid, through the interface toward the air current)]

Mathematically, this can be expressed as:

$$h_l a_{\text{ev}}(T_{I.\text{ev}} - T_{l.\text{ev}}) = h_g a_{\text{ev}}(T_{I.\text{ev}} - T_{g.\text{ev}}) + \lambda_o K_m a_{\text{ev}}(W_{I.\text{ev}} - W_{g.\text{ev}}) \quad (3)$$

At the air–water interface, the mass balance is given by the following equation:

[Quantity of steam accumulated] = [(Mass water quantity transferred from the interface through the air film toward air current during dt) – (Quantity of steam transmitted to air current during the same interval dt)]

$$\frac{\partial W_{g.\text{ev}}}{\partial t} = -\frac{m_{g.\text{ev}}}{M_{g.\text{ev}}}\frac{\partial W_{g.\text{ev}}}{\partial z} + \frac{K_m a_{\text{ev}}}{M_{g.\text{ev}}}\left(W_{I.\text{ev}} - W_{g.\text{ev}}\right) \quad (4)$$

4.2. Dehumidification process

4.2.1. Water phase

[Quantity of energy accumulated in the element of volume of height dz] = [(Quantity of heat transmitted from air–water interface to water in the condenser during the interval of time dt) – (Quantity of heat carried away by water during the interval of time dt)]

Mathematically, this can be expressed as:

$$\frac{\partial T_e}{\partial t} = -\frac{D_e}{M_e}\frac{\partial T_e}{\partial z} + \frac{UA_c}{M_e C_e}\left(T_{\text{Ic}} - T_e\right) \quad (5)$$

4.2.2. Air phase

[Quantity of energy accumulated in the element of volume of height dz] = [(Quantity of heat carried away by air during the interval of time dt) – (sensible heat quantity transmitted toward the surface of separation air–water during dt) – (latent heat quantity due to the condensation of steam transmitted to the surface of separation air–water during dt)]

Mathematically, this can be expressed as:

$$\frac{\partial T_{\text{gc}}}{\partial t} = \frac{m_{\text{gt}}}{M_{\text{gc}}}\frac{\partial T_{\text{gc}}}{\partial z} - \frac{h_{\text{gc}} A_c}{M_{\text{gc}} C_{\text{gc}}}\left(T_{\text{gc}} - T_{\text{Ic}}\right) - \frac{\lambda_o K_{\text{mc}} A_c}{M_{\text{gc}} C_{\text{gc}}}\left(W_{\text{gc}} - W_{\text{Ic}}\right) \quad (6)$$

4.2.3. Air–condensate interface

The heat balance at air–condensate interface is given by the following equation:

[(Cooling sensible heat quantity of humid air received by air–condensate interface) + (latent heat quantity liberated during the condensation at air–condensate interface)] = [Quantity of heat transmitted from air–condensate interface to the cooling water]

Mathematically, this can be expressed as:

$$h_{\text{gc}} A_c\left(T_{\text{gc}} - T_{\text{Ic}}\right) + UA_c\left(T_{\text{Ic}} - T_e\right) = \lambda_o K_{\text{mc}} A_c\left(W_{\text{gc}} - W_{\text{Ic}}\right) \quad (7)$$

The mass balance at air–condensate interface is given by the following equation:

[Accumulated humid air quantity] = [(Quantity of air transferred toward air–water interface during interval dt) – (Quantity of steam condensed during the same interval dt)]

Mathematically, this can be expressed as:

$$\frac{\partial W_{\text{gc}}}{\partial t} = \frac{m_{\text{gt}}}{M_{\text{gc}}}\frac{\partial W_{\text{gc}}}{\partial z} + \frac{K_{\text{mc}} A_c}{M_{\text{gc}}}\left(W_{\text{gc}} - W_{\text{Ic}}\right) \quad (8)$$

5. Model approximation of the distillation module

The obtained set of partial derivative equations with distributed parameters is transformed to the following set of ordinary differential equations using the functional approximation method of orthogonal collocation with the boundary conditions [12,17,18]: $0 \le z \le H$, $T_{l.\mathrm{ev}}(H,t) = T_{l1,\mathrm{ev}}(t)$, $T_e(0,t) = T_{e1}(t)$, $T_{g.\mathrm{ev}}(0,t) = T_{g1,\mathrm{ev}}(t)$, $T_{\mathrm{gc}}(H,t) = T_{\mathrm{gc1}}(t)$ and $W_{g.\mathrm{ev}}(0,t) = W_{g1,\mathrm{ev}}(t)$, $W_{\mathrm{gc}}(H,t) = W_{\mathrm{gc1}}(t)$.

The expression of the distillation module-reduced dynamic model is given by the following equations:

$$\frac{\mathrm{d}T_{l.\mathrm{ev}i}}{\mathrm{d}t} = \frac{m_l}{M_{l.\mathrm{ev}}}\left[\sum_{j=0}^{N} l_{ij} T_{l,\mathrm{ev}j} + l_{i\mathrm{N}+1} T_{l,\mathrm{ev}2}\right] - \frac{h_l a_{\mathrm{ev}}}{M_{l.\mathrm{ev}} C_l}\left(T_{I.\mathrm{ev}} - T_{l.\mathrm{ev}i}\right) \tag{9}$$

$$\begin{aligned}\frac{\mathrm{d}T_{g.\mathrm{ev}i}}{\mathrm{d}t} &= -\frac{m_{g.\mathrm{ev}}}{M_{g.\mathrm{ev}}}\left[\sum_{j=1}^{N+1} l_{ij} T_{g,\mathrm{ev}j} + l_{i0} T_{g,\mathrm{ev}0}\right] \\ &\quad -\frac{h_g a_{\mathrm{ev}}}{M_{g.\mathrm{ev}} C_{g.\mathrm{ev}}}\left(T_{g.\mathrm{ev}i} - T_{I.\mathrm{ev}}\right)\end{aligned} \tag{10}$$

$$\begin{aligned}\frac{\mathrm{d}W_{g.\mathrm{ev}i}}{\mathrm{d}t} &= -\frac{m_{g.\mathrm{ev}}}{M_{g.\mathrm{ev}}}\left[\sum_{j=1}^{N+1} l_{ij} W_{g.\mathrm{ev}j} + l_{i0} W_{g.\mathrm{ev}0}\right] \\ &\quad +\frac{K_m a_{\mathrm{ev}}}{M_{g.\mathrm{ev}}}\left(W_{I.\mathrm{ev}} - W_{g.\mathrm{ev}i}\right)\end{aligned} \tag{11}$$

$$h_l a_{\mathrm{ev}}(T_{I.\mathrm{ev}} - T_{l.\mathrm{ev}i}) = h_g a_{\mathrm{ev}}(T_{I.\mathrm{ev}} - T_{g.\mathrm{ev}i}) + \lambda_o K_m a_{\mathrm{ev}}(W_{I.\mathrm{ev}} - W_{g.\mathrm{ev}i}) \tag{12}$$

$$\frac{\mathrm{d}T_{\mathrm{e}i}}{\mathrm{d}t} = -\frac{D_e}{M_e}\left[\sum_{j=1}^{N+1} l_{ij} T_{\mathrm{e}i} + l_{i0} T_{\mathrm{e}1}\right] + \frac{UA_c}{M_e C_e}\left(T_{\mathrm{Ic}} - T_{\mathrm{e}i}\right) \tag{13}$$

$$\begin{aligned}\frac{\mathrm{d}T_{\mathrm{gc}i}}{\mathrm{d}t} &= \frac{m_{\mathrm{gt}}}{M_{\mathrm{gc}}}\left[\sum_{j=0}^{N} l_{ij} T_{\mathrm{gc}i} + l_{iN+1} T_{\mathrm{gc}2}\right] - \frac{h_{\mathrm{gc}} A_c}{M_{\mathrm{gc}} C_{\mathrm{gc}}}\left(T_{\mathrm{gc}i} - T_{\mathrm{Ic}}\right) \\ &\quad -\frac{\lambda_o K_{\mathrm{mc}} A_c}{M_{\mathrm{gc}} C_{\mathrm{gc}}}\left(W_{\mathrm{gc}i} - W_{\mathrm{Ic}}\right)\end{aligned} \tag{14}$$

$$\frac{\mathrm{d}W_{\mathrm{gc}i}}{\mathrm{d}t} = \frac{m_{\mathrm{gt}}}{M_{\mathrm{gc}}}\left[\sum_{j=0}^{N} l_{ij} W_{\mathrm{gc}i} + l_{iN+1} W_{\mathrm{gc}2}\right] + \frac{K_{\mathrm{mc}} A_c}{M_{\mathrm{gc}}}\left(W_{\mathrm{gc}i} - W_{\mathrm{Ic}}\right) \tag{15}$$

$$h_{\mathrm{gc}} A_c\left(T_{\mathrm{gc}i} - T_{\mathrm{Ic}}\right) + UA_c\left(T_{\mathrm{Ic}} - T_{\mathrm{e}i}\right) = \lambda_o K_{\mathrm{mc}} A_c\left(W_{\mathrm{gc}i} - W_{\mathrm{Ic}}\right) \tag{16}$$

$$\frac{\mathrm{d}m_c}{\mathrm{d}z} = K_{\mathrm{mc}} A_c\left(W_{\mathrm{Ic}} - W_{\mathrm{gc}i}\right) \tag{17}$$

where $i = 1, 2, 3, \ldots, N + 1$.

6. Results and discussion

In this section, we present the numerical results obtained when subjecting the model of the distillation module to various inputs, such as operating conditions, to determine how it behaves and thus predict the characteristics of the actual distillation system. Figs. 5 and 6 show the variation of the amount of evaporated water, m_{ev}, inside the distillation module as a function, respectively, of water and air inlet temperatures for different values of air flow rates. Results depicted in Fig. 5 show that the amount of evaporated water increases with increasing inlet water temperature and air flow rate. This can be explained by the fact that increasing inlet water temperature increases the gradient temperature between air and water inside the distillation module which, in its turn, leads to increase the mass and heat transfer coefficients and then the amount of evaporated water. These results were also obtained by Brendel [19] and Al-Hallaj [20] who showed experimentally that the loading of air with water vapor increases with the water temperature entering the humidification process. Fig. 6 shows the evolution of the evaporated water amount in function of air temperature and air flow rate which will be condensed in the dehumidification chamber. The first thing that can be drawn from this figure is that, the amount of evaporated water increases proportionally with increase of air flow rate which varies between 0.02 and 0.06 kg/s and inlet air temperature. The curves vary in a progressive manner up to a certain inlet air temperature value

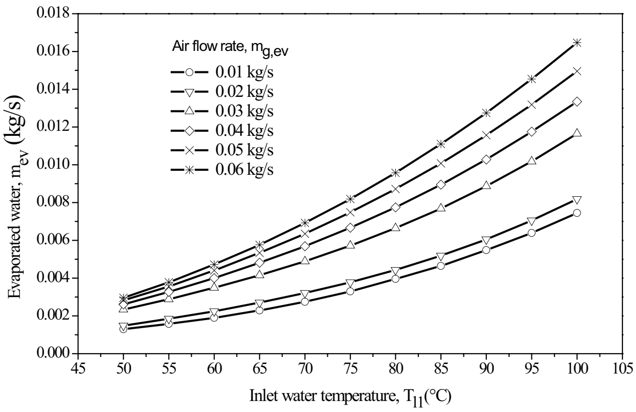

Fig. 5. Variation of evaporated amount of water vs. inlet water temperature and air flow rate.

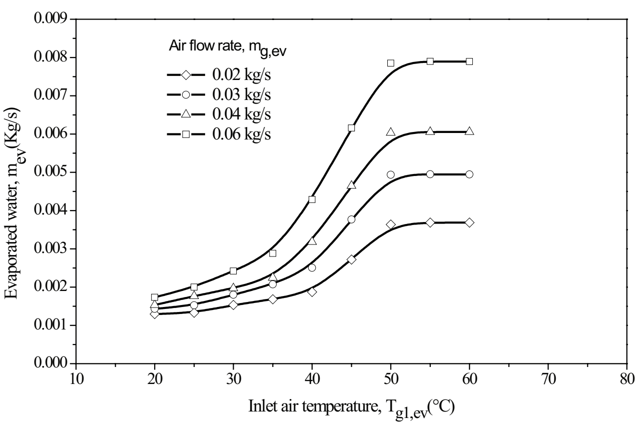

Fig. 6. Variation of evaporated amount of water vs. inlet air temperature and air flow rate.

and then remain constant. Similarly, Chafik [21] showed theoretically that humidification increases with the inlet air temperature. This result can be explained as follows: the increase of air temperature inside the humidification chamber increases its capacity to load water vapor thus resulting in high amount of evaporated water. From Fig. 6, it is clear that beyond 55°C the air temperature has no influence on air humidification; this means that air reaches its saturated state.

To estimate the thermal performance of the humidification process, efficiency is used. It is defined as the ratio between the difference between the humidity ratio at the exit and the inlet of the humidifier and difference when the exit air is saturated as reported in studies by Chafik [21], Orfi et al. [22] and Agricultural University of Athens [23] and given by the following:

$$\varepsilon = \frac{W_{g2\cdot ev} - W_{g1\cdot ev}}{W_{I\cdot ev} - W_{g1\cdot ev}} \tag{18}$$

where $W_{g1\cdot ev}$ and $W_{g2\cdot ev}$ are, respectively, the absolute humidity of air at the inlet and the outlet of the evaporator. $W_{I\cdot ev}$ is the saturation humidity corresponding to the actual humidification process. Figs. 7 and 8 present the variation of the humidification efficiency, ε, and the amount of evaporated water, m_{ev}, as a function of operating parameters. Fig. 7 shows the variation of distillation module humidification efficiency vs. inlet water temperature at the humidification chamber for different values of water flow rates. It is clear from the obtained curves that increasing the humidifier inlet water temperature decreases the values of humidification efficiency. In fact, the increase of water temperature at the inlet of the humidifier, and consequently the air temperature during humidification process leads to increase in the air bearing capacity of moisture. Consequently, the air leaving the humidifier is far from saturation point for a given moisture mass transfer and thus decreases the humidification efficiency as displayed in Fig. 7. The obtained result shows good agreement with the result reported by Ahmed et al. [24]. Also the figure shows that increasing water flow rates increase the humidification efficiency. This result is due to the fact that higher water flow rate will improve both mass transfer rate and the degree of wetting of packing [25]. The air humidity at the inlet of the humidifier is the output of the dehumidification chamber. So, its value is variable. Therefore, it is interesting to perceive the influence of this parameter on the distillation module performance. Variations of evaporated water amount and humidification efficiency vs. inlet absolute air humidity are depicted in Fig. 8. The presented curves show that increasing inlet absolute air humidity decreases the amount of evaporated water and the humidification efficiency. In fact, the increase of air humidity at the humidifier inlet decreases the capacity of air to load water vapor and thus decreases the difference of humidity ratio between the inlet and the exit of the humidifier where the exit air may not reach its saturated state. Consequently, the humidification efficiency decreases. The obtained results show excellent agreement with the work of Ben Amara [26].

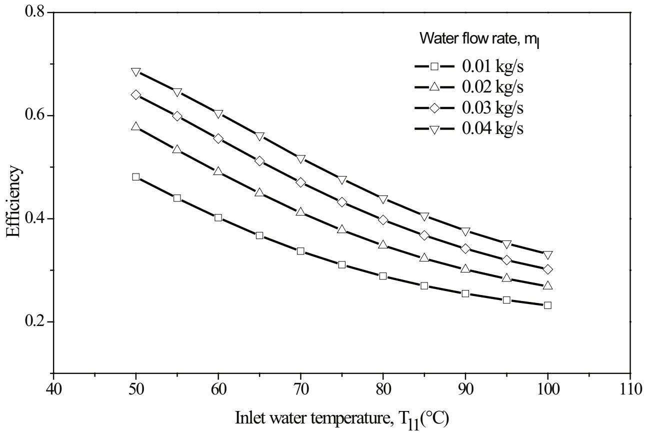

Fig. 7. Variation of distillation module efficiency vs. inlet water temperature and water flow rate.

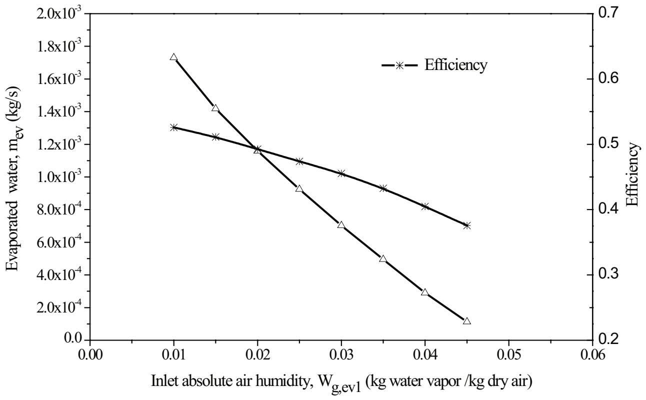

Fig. 8. Variations of evaporated amount of water and humidification efficiency vs. inlet absolute air humidity.

7. Conclusion

This paper deals with the theoretical study of a distillation module used in solar desalination unit using the HD principle. The first part of the study deals with the presentation of the designed and constructed distillation module. In the second part, a mathematical model based on heat and mass balances for air and water inside the distillation module is presented. The developed model is simulated using the Borland C++ software to study the influence of operating parameters, namely: the air and water mass flow rates, the inlet air humidity, the inlet water temperature and the inlet air temperature on both the humidification efficiency of the distillation module and the amount of evaporated water. The obtained results are in good agreement with the results reported in previous research works. According to section 6, to ensure a good performance of the distillation module, it is interesting to work with high values of both air and water temperatures and low values of air humidity at the inlet of the humidifier to allow the latter to provide high values of evaporated water rate.

Symbols

A	—	Air–water exchanger area in the condensation tower, m^2
a	—	Air–water exchanger area, m^2
C_e	—	Water specific heat, J/(kg K)
C_f	—	Fluid specific heat, J/(kg K)
C_g	—	Moist air specific heat in the humidifier, J/(kg K)
C_{gc}	—	Moist air specific heat in the condensation tower, J/(kg K)
$C_{g,ev}$	—	Moist air specific heat in the evaporation tower, J/(kg K)
D_e	—	Water mass velocity in the condensation tower, kg/(m^2 s)
h	—	Heat transfer coefficient, J/(kg K)
h_g	—	Air heat transfer coefficient at the air–water interface, W/(m^2 K)
h_e	—	Water heat transfer coefficient at the air–water interface, W/(m^2 K)
K	—	Thermal conductivity, W/(m K)
K_m	—	Water vapor mass transfer coefficient at the air–water interface, kg/(m^2 s)
m	—	Mass flow rate, kg/s
m_c	—	Fresh water production, kg/s
m_{gt}	—	Total mass velocity of moist air in the condenser, kg/(m^2 s)
T	—	Temperature, K
T_1	—	Temperature at the air–water interface, K
T_x	—	Temperature of liquid at bulk, K
T_v	—	Temperature of gas at bulk, K
U	—	Overall heat transfer coefficient in the condensation tower, W/(m^2 K)
W	—	Air humidity, kg water/kg dry air
W_1	—	Saturation humidity, kg water/kg dry air
Z	—	Coordinate in the flow direction, m

Greek

λ_o	—	Latent heat of water evaporation, J/kg

Subscripts

1	—	Tower bottom
2	—	Tower top
a	—	Air
c	—	Condensation tower
e	—	Cooling water
ev	—	Evaporation tower
g	—	Moist air
l	—	Liquid
I	—	Interface

Acknowledgments

The authors wish to thank the Ministry of Higher Education, Scientific Research and Information and Communication Technologies MESRS-TIC for its financial support to the R&D project entitled “Solar Driven membrane distillation for resource efficient desalination in remote areas”, and the Fraunhofer Institute for Solar Energy Systems ISE for its collaboration.

References

[1] J.J. Hermosillo, C.A. Arancibia-Bulnes, C.A. Estrada, Water desalination by air humidification: mathematical model and experimental study, Solar Energy, 86 (2012) 1070–1076.
[2] A.F. Mashaly, A.A. Alazba, A.M. Al-Awaadh, Assessing the performance of solar desalination system to approach near-ZLD under hyper arid environment, Desal Wat. Treat., 57 (2016) 12019–12036.
[3] A.A. Attia, Thermal analysis for system uses solar energy as a pressure source for reverse osmosis (RO) water desalination, Solar Energy, 86 (2012) 2486–2493.
[4] M.T. Ghazal, U. Atikol, F. Egelioglu, An experimental study of a solar humidifier for HDD systems, Energy Convers. Manage., 82 (2014) 250–258.
[5] C. Muthusamy, K. Srithar, Energy and exergy analysis for a humidification–dehumidification desalination system integrated with multiple inserts, Desalination, 367 (2015) 49–59.
[6] E.W. Tow, J.H. Lienhard V, Experiments and modeling of bubble column dehumidifier performance, Int. J. Therm. Sci., 80 (2014) 65–75.
[7] M.H. Sharqawy, H. Liu, The effect of pressure on the performance of bubble column dehumidifier, Int. J. Heat Mass Transf., 87 (2015) 212–221.
[8] M. Sievers, J.H. Lienhard V, Design of plate-fin tube dehumidifiers for humidification–dehumidification desalination systems, Heat Transfer Eng., 36 (2015) 223–243.
[9] M.A. Kassim, B. Benhamou, S. Harmand, Effect of air humidity at the entrance on heat and mass transfers in a humidifier intended for a desalination system, Appl. Therm. Eng., 31 (2011) 1906–1914.
[10] K. Bourouni, M.T. Chaibi, Modelling of heat and mass transfer in a horizontal-tube falling film condenser for brackish water desalination in remote areas, Desalination, 166 (2004) 17–24.
[11] S. Yanniotis, K. Xerodemas, Air humidification for seawater desalination, Desalination, 158 (2003) 313–319.
[12] K. Zhani, H. Ben Bacha, T. Damak, Modeling and experimental validation of a humidification and dehumidification desalination unit solar part, Energy 36 (2011) 3159–3169.
[13] K. Zhani, H. Ben Bacha, Modeling, simulation and experimental validation of a pad humidifier used in solar desalination process, Desal. Wat. Treat., 51 (2013) 1477–1486.
[14] K. Bourouni, M.T. Chaibi, L. Tadrist, Water desalination by humidification and dehumidification of air: state of the art, Desalination, 137 (2001) 167–176.
[15] W. Abdelmoez, M.S. Mahmoud, T.E. Farrag, Water desalination using humidification/ dehumidification (HDH) technique powered by solar energy: a detailed review, Desal. Wat. Treat., 52 (2014) 4622–4640.
[16] J.C. Geankoplis, Transport Processes and Unit Operation, Prentice-Hall International Inc., 3rd ed., 1993, pp. 602–605.
[17] T. Damak, Modelling, Evaluation and Command of Biotechnical Processes of Hyperbolic Type, PhD Thesis, Universite Paul Sabatier, Toulouse, France, 1994.
[18] R.K. Srivastava, B. Joseph, Reduced-order model for separation columns. V. Selection of collocation points, Comput. Chem. Eng., 9 (1985) 601–613.
[19] T. Brendel, Solare Meewasserental sungsanlagen mit mehrstufiger verdungtung, Phd Thesis, Ruhr University Bochum, Germany, 2003.
[20] S. Al-Hallaj, Solar Desalination By Humidification-Dehumidification Cycle, MSc Thesis, Jordan University of Science and Technology, Jordan, 1994.
[21] E. Chafik, A new sea water desalination process using solar energy, Desalination, 153 (2002) 25–37.
[22] J. Orfi, M. Laplante, H. Marmouch, N. Galanis, B. Benhamou, S. Ben Nasrallah, C.T. Nguyen, Experimental and theoretical study of a humidification–dehumidification water desalination system using solar energy, Desalination, 168 (2004) 151–159.
[23] Agricultural University of Athens, 10th Deliverable: Experimental Optimization of Humidifiers Design of an Optimized Humidifier Prototype, EU Contract No. IC18-CT98-0265, January 2001.

[24] H.A. Ahmed, I.M. Ismail, F. Wael Saleh, M. Ahmed, Experimental investigation of humidification-dehumidification desalination system with corrugated packing in the humidifier, Desalination, 410 (2017) 19–29.
[25] N.K. Nawayseh, M.M. Farid, S. Al-Hallaj, A.R. Tamimi, Solar desalination based on humidification process. Part I. Evaluating the heat and mass transfer coefficients, Energy Convers. Manage., 40 (1999) 1423–1439.
[26] M. Ben Amara, Etude du dessalement d'eau par Humidification - Déshumidification de l'air, PhD Thesis, Faculté des Sciences de Tunis, Université de Tunis El-manar, 2005.